Evidence for a Cosmological Constant and for the Expansion of the Universe*

GERSON GOLDHABER for the Supernova Cosmology Project†
Institute for Nuclear and Particle Astrophysics
Lawrence Berkeley National Laboratory
& Center for Particle Astrophysics
University of California at Berkeley
Berkeley, California 94720
gerson@lbl.gov

*This work was supported in part by the United States Department of Energy, contract numbers DE-AC03-76SF00098, CfPA, and NSF contract number AST-9120005.

†G. Aldering,[a] B. J. Boyle,[b] P. G Castro,[a] W. J. Couch,[c] S. Deustua,[a] S. Fabbro,[d] R. S. Ellis,[e] A. V. Filippenko,[f] A. Fruchter,[g] G. Goldhaber,[a] A. Goobar,[h] D. E. Groom,[a] I. M. Hook,[i] M. Irwin,[e] A. G. Kim,[j] M. Y. Kim,[a] R. A. Knop,[a] J. C. Lee,[e] T. Matheson,[f] R. G. McMahon,[e] H. J. M. Newberg,[n] C. Lidman,[o] P. Nugent,[a] N. J. Nunes,[a] R. Pain,[d] N. Panagia,[g] C. R. Pennypacker,[a] S. Perlmutter,[a] R. Quimby,[a] P. Ruiz-Lapuente,[k] B. Schaefer,[l] and N. Walton.[m] (*a*) LBNL, Berkeley, California, USA, (*b*) Anglo-Australian Observatory, Sydney, Australia, (*c*) University of New South Wales, Sidney, Australia, (*d*) LPNHE, CNRS-IN2P3, University of Paris VI & VII, Paris, France, (*e*) Institute of Astronomy, Cambridge, United Kingdom, (*f*) Dept. of Astronomy, Univ. of California, Berkeley, USA, (*g*) Space Telescope Science Inst., Baltimore, Maryland, USA, (*h*) Dept of Physics, Stockholm Univ., Sweden, (*i*) Inst. of Astronomy, Univ. of Edinburgh United Kingdom, (*j*) L.P.C.C. College de France, Paris, France, (*k*) Dept. of Astronomy, Univ. of Barcelona, Spain, (*l*) Dept. of Astronomy, Yale Univ., New Haven, Connecticut, USA, (*m*) Isaac Newton Group, La Palma, Spain, (*n*) FNAL, Batavia, Illinois, USA, (*o*) ESO, La Scilla, Chile.

ABSTRACT

A search for cosmological supernovae has discovered over 75, most of which are type Ia supernovae (SNe Ia). There is strong evidence from measurements of nearby type Ia supernovae that they can be considered as distance indicators or "standard candles" after correction for the width (time-scale stretch parameter) of the individual light curves. Measurements and analysis are completed on 42 of these distant, $z = 0.18$ to 0.83, supernovae. These supernovae, together with 18 "nearby" $z < 0.11$ supernovae from the Calán/Tololo Supernova Survey, allow us to measure the ratio of the matter density of the universe to the critical density Ω_M, together with the normalized cosmological constant Ω_Λ, the energy density of the vacuum. For a flat universe, i.e., $\Omega_M + \Omega_\Lambda = 1$, we obtain $\Omega_M = 0.28\ ^{+0.09}_{-0.08}(stat.)\ ^{+0.05}_{-0.04}(syst.)$. The data are strongly inconsistent with a $\Lambda = 0$ flat cosmology, the simplest inflationary universe model. An open, $\Lambda = 0$ cosmology also does not fit the data well: the data strongly suggest that the cosmological constant is nonzero and positive, with a confidence of $P(\Lambda > 0) > 99\%$. By treating 36 of our high-z SNe Ia with $0.30 < z < 0.70$ as a group, we find that the expected light curve widths, based on the nearby width distribution, are in agreement with the observed distribution. In particular, we demonstrate that when normalized, our SNe fit a single curve with a single parameter stretch, s. We also obtain a direct confirmation of the hypothesis that extragalactic redshifts are due to cosmological expansion by observing the expected "time dilation" Doppler shift $1 + z$ of SNe Ia light curves at high redshift.

1. The Matter Density and Vacuum Energy Density of the Universe

When Einstein introduced his General Theory of Relativity (1916) the universe was assumed to be static. To accomplish such a static universe, Einstein had to introduce a repulsive force corresponding to a "cosmological constant," Λ, to compensate for the gravitational attraction of the matter in the universe. Later, when Hubble discovered that the universe was actually expanding (1924), Einstein called the cosmological constant "his greatest mistake." All the same, since Λ is consistent with Einstein's theory, one need not assume that $\Lambda = 0$. Thus, the value of Λ becomes an experimental question. Here Ω_Λ, the vacuum energy density, is given by $\Omega_\Lambda = \Lambda/(3H_0^2)$ and Ω_M is the matter density of the universe. In our current study, we primarily obtain a linear combination of these two densities.

When we started out with this study ten years ago, we were planning to measure the deceleration of the universe q_0. On the then prevalent assumption (prejudice) that $\Omega_\Lambda = 0$, we expected a positive deceleration of the universe due to matter density. With our present observations we find, to a high probability $P(\Lambda > 0) > 99\%$, that q_0 is actually negative, corresponding to an acceleration of the expansion of the universe! Our best fit corresponds to the relation $0.8\Omega_M - 0.6\Omega_\Lambda \approx -0.2 \pm 0.1$. For a flat cosmology, $\Omega_M + \Omega_\Lambda = 1$, this corresponds to $\Omega_M = 0.28\ ^{+0.09}_{-0.08}(stat.)\ ^{+0.05}_{-0.04}(syst.)$.

Before our present work started, estimates of Ω_M, based on a variety of experiments, ranged from 0.05 to 1.5. Since the light emitting matter contributes roughly 0.01 to Ω_M, a measurement of Ω_M also determines the contribution of dark matter to the universe.

2. Type Ia SNe as Calibrated Standard Candles?

There is good evidence that type Ia supernovae (SNe Ia), the brightest of all the different types of SNe, can be calibrated to have a standard brightness. A plausible explanation for this behavior is that SNe Ia are the consequence of the explosion of a white dwarf star as it approaches a critical mass of 1.4 solar masses, the Chandrasekhar limit.

A white dwarf is a star that has burnt all of its hydrogen and helium by fusion primarily to carbon and oxygen, and as a result has collapsed under the gravitational force to a degenerate electron gas in which the C and O nuclei are embedded. The white dwarf thus has the mass of the order of the mass of the sun, but a radius comparable to that of the earth. If this white dwarf is in a binary system with another star, a common occurrence, the companion star can transfer matter to the white dwarf until it approaches the Chandrasekhar limit. Near this mass, the electron degeneracy pressure can no longer support the star and a runaway thermonuclear explosion occurs.

In this supernova explosion, the temperature and density reach the point at which the C and O nuclei fuse and produce higher mass nuclei. The fusion process stops at ^{56}Ni, a radioactive isotope with an equal number of protons and neutrons. In fact, an enormous amount of ^{56}Ni is produced, typically 0.6 of a solar mass. In the explosion, the newly produced material is ejected with velocities of about 10,000 km/sec to 30,000 km/sec. At first, the exploding star is too small to be seen. Over a period of a few days, however, it expands rapidly and its brightness reaches a maximum value, in about 18 days, in the rest system. It is during this period that we first discover the SN as we will describe below. The light observed is produced by ionization from the decay products of ^{56}Ni and its daughter isotope ^{56}Co. The ^{56}Ni isotope has a half-life of about six days and ^{56}Co has a half-life of 77 days, so it is primarily the ^{56}Co decay that is powering the supernova at maximum light. Finally, ^{56}Co decays to stable ^{56}Fe.

All the same, not all SNe Ia have exactly the same brightness at the peak of the light curve. There is a dispersion of about 0.24 to 0.5 magnitudes (depending on the sample selection criteria) in the maximum brightness distribution.[1] Phillips[2] noted a correlation between the brightness and the decline rate of the SNe Ia. We express this correlation (Perlmutter *et al.*, 1997, Ref. 3) in terms of a stretch parameter s applied to the time axis in the light curve of the SN. Thus, s affects both the rise rate and the decline rate of the SN. The greater s, meaning the wider the SN light curve, with reference to the standard Leibundgut[4] curve, the brighter it is. We measure typical values for s from 0.8 to 1.2 with a few outliers above and below these values. We find a correction to the B-band absolute magnitude M of $-\alpha(s-1)$. In our analysis, we apply this correction to the apparent magnitude m_B giving an effective magnitude $m_B^{\text{effective}} = m_B + \alpha(s-1)$, which then corresponds to a unique value of the absolute magnitude M with an uncertainty of approximately 0.17 magnitudes or ~17% in flux. (This dispersion can be improved still further with multiple filter-band constraints on extinction; see discussions in Perlmutter *et al.*[5] and references therein.) In theoretical models, it has been suggested that this light curve width-luminosity relation can be understood in terms of varying amounts of ^{56}Ni produced, and hence, variation in the temperature of the ejecta.

3. The Observation of 42 SNe

In an ongoing systematic search we have, over the last six years, discovered and studied 75 SNe. The majority of these were the most distant SNe ever observed. We have now completed the analysis of 42 of these SNe. The analysis of the first seven of our SNe has already been published (Perlmutter, 1997).[3] An additional SN at $z = 0.83$ has been measured with the Hubble Space Telescope and added to this sample (Perlmutter, 1998a, Ref. 6). The first analysis of a 40-supernova sample was presented at the January 1998 meeting of the American Astronomical Society (Perlmutter, 1998b, Ref. 7); The current, more extensive analysis[5] agrees with those results—as well as with a subsequent analysis of 16 SNe by the Hi-Z Supernova Search Team (Riess *et al.* 1998).[8]

When we began our program, only one high-redshift supernova had been discovered (18 days past maximum).[9] We developed a technique that made it possible to discover *batches* of high-redshift supernovae, while still on the rise to maximum light in a systematic, predictable way. About twice a year, during two sets of two nights at the telescope, our procedure is to take about 50–70 different CCD images, depending on the depth in redshift we are trying to achieve. Each image covers about 15 × 15 square minutes of arc on the sky. The total area covered is thus about 3-4 square degrees. The first set of images are considered as "reference" images. The second set observed about three weeks later, are the "search" images in which we hunt for the new light due to a supernova. The timing relative to the moon is critical, since we deal with such dim objects that they are difficult to observe at or near full moon. We take our reference images just after the new moon and our search images just before the next new moon. After the discovery, we take follow-up images of the SNe as well as the spectra.

The new supernova in this sample of 42 were all discovered while still brightening, using the Cerro Tololo four-meter telescope with the 2048^2 prime-focus CCD camera or the 4×2048^2 big throughput camera. The supernovae were followed with photometry over the peak of their light curves, and approximately two to three months further (~ 40–60 days in their restframe) using the CTIO 4-m, WIYN 3.6-m, ESO 3.6-m, INT 2.5-m, and WHT 4.2-m telescopes. (SN 1994ap and other more recent supernovae have also been followed with HST photometry.) The supernova redshifts and spectral identifications were obtained using the

Keck I and II 10-m telescopes with LRIS and the ESO 3.6-m telescope. We have observed spectra of the host galaxies for all of these. SNe spectra were observed for almost all SNe after the first six SNe. The photometry coverage was most complete in Kron-Cousins R-band, with Kron-Cousins I-band photometry coverage ranging from two or three points near peak to relatively complete coverage paralleling the R-band observations.

4. The Light Curve and K-Corrections

We compare our measurements to nearby SN light curves measured with a blue filter. Because of the large redshift, the spectral features captured in the blue filter appear in the "red." We thus carry out our measurements with a red filter and then translate our measurements into the blue. As it turned out, this correction—called a K-correction—was particularly straightforward for our first distant SN because $1 + z = 1.458$ gives the ratio of the redshifted wavelength to the wavelength at emission. This value turned out to be the ratio of the central wavelength transmitted by our red filter to that of the blue filter, used for the nearby standard light curve. The acceptance width of the two filters were also roughly in this same ratio. For other z values the K-correction is a function of the epoch on the light curve and the stretch. The procedure modifies the light curve to allow for changes in the portion of the spectrum captured by each filter, Kim *et al.*[11] and Nugent *et al.*[12]

5. Our Method for Obtaining Ω_M and Ω_Λ

Our method for obtaining both Ω_M and Ω_Λ is discussed in Perlmutter *et al.*[3,6] and Goobar and Perlmutter.[13]

To obtain Ω_M and Ω_Λ, we make use of the following measurements:

- The redshift of the supernova, or parent galaxy, z is related to the wavelength change $\lambda - \lambda_o$ of the receding object. Here, z is defined as $z = (\lambda - \lambda_o)/\lambda_o$ and λ_o is the wavelength in the rest system, while λ is the measured wavelength for identified lines. This requires taking a spectrum of the SN to identify type Ia SN whenever possible, as well as of the galaxy, for an accurate redshift determination.
- The apparent magnitude m_B of the high-redshift SN at the peak of its light curve, calibrated to a standard light curve width ($s = 1$). This is based on the measurement of the SN light intensity as a function of time (generally in two filters), the photometry calibration, K-corrections, and a fit to the light curve to obtain the peak brightness and the light-curve width s. (The two-filter measurements make it possible to characterize the extinction due to dust that reddens the light.)
- The same measurements obtained for a group of 18 well-measured nearby Type Ia SNe from the Calán/Tololo Supernova Survey.[14–16]

The relation between the measured apparent magnitude m_R and the absolute magnitude M_B for type Ia SN, is given by

$$m_R = 5 \log D_L + M_B + 25 + K_{RB}. \quad (1)$$

Here, K_{RB} is the K-correction factor between red and blue SNe magnitudes and $D_L = D_L(z; \Omega_m, \Omega_\Lambda, H_o)$ is the luminosity distance given in Mpc (≈ 3 million light years). Here, H_o is the Hubble constant, c the velocity of light, z is the measured redshift, usually obtained from the spectrum of the host galaxy. At first sight it appears that D_L depends on the Hubble constant H_o as well. However, it turns out that the Hubble constant cancels because H_o also appears in the determination of M_B obtained from type Ia SN measurements in nearby galaxies Hamuy *et al.*[14–16]

Figure 1 shows $m_B^{\text{effective}}$ for our 42 SNe, as well as the 18 Calán/Tololo Supernova Survey SNe, plotted against redshift. The curves represent the Hubble diagram for a variety of cosmological models as indicated on the figure. The fit to the expression for D_L gives an approximately linear relation between Ω_M and Ω_Λ in the region of interest ($\Omega_M < 1.5$). Our best fit is illustrated in Fig. 2. We have carried out a series of fits under somewhat different data selections, e.g., (a) all the data, (b) with two outlying SNe removed, (c) with two reddened and two extreme stretch SNe removed, etc. (see, Perlmutter *et al.*, 1998c, for details).[5] Our results are quite stable with respect to these various sample selections. In particular, one fit was made with *no* stretch corrections, and this yielded a fit completely consistent with our results *with* stretch corrections. We have used the

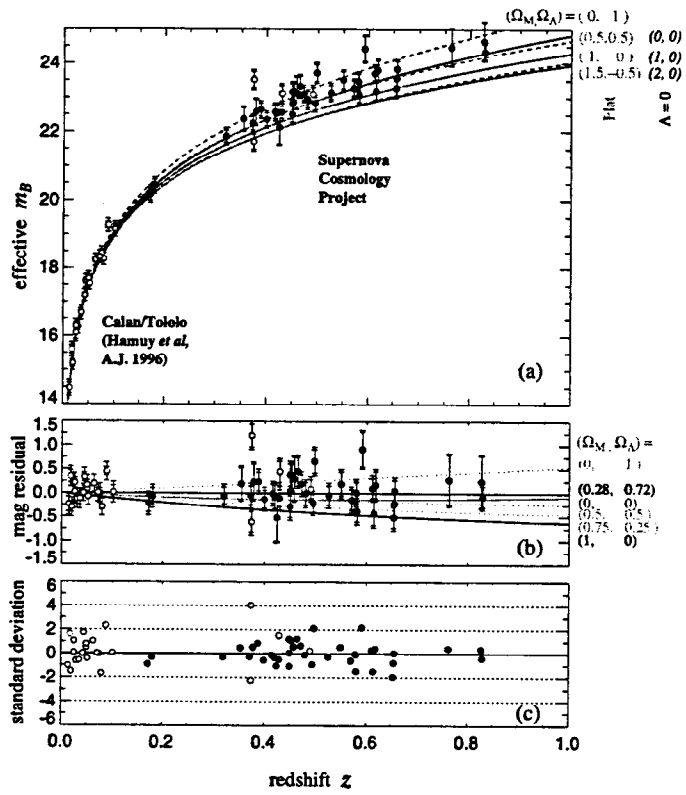

Figure 1: (a) Hubble diagram for 42 high-redshift SNe Ia from the Supernova Cosmology Project, and 18 low-redshift SNe Ia from the Calán/Tololo Supernova Survey, after correcting both sets for the SN Ia light curve width-luminosity relation. The inner error bars show the uncertainty due to measurement errors, while the outer error bars show the total uncertainty when the intrinsic luminosity dispersion, 0.17 mag, of light curve-width-corrected SNe Ia is added in quadrature. The unfilled circles indicate supernovae not included in Fit C. The solid curves are the theoretical $m_B^{\text{effective}}(z)$ for a range of cosmological models with zero cosmological constant as indicated on the figure. (b) The magnitude residuals from the best-fit flat cosmology for the Fit C supernova subset, $(\Omega_M, \Omega_\Lambda) = (0.28, 0.72)$. The curves are for a range of flat cosmological models as indicated on the figure. (c) The uncertainty-normalized residuals from the best-fit flat cosmology for the Fit C supernova subset, $(\Omega_M, \Omega_\Lambda) = (0.28, 0.72)$.

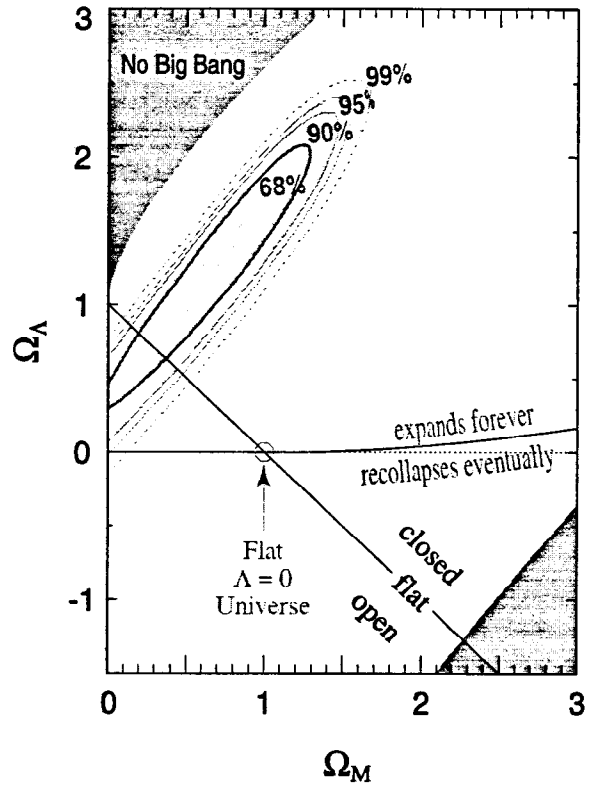

Figure 2: The 68%, 90%, 95%, and 99% confidence regions in the Ω_M–Ω_Λ plane from Perlmutter *et al.*[6] (see this reference for details of the fit procedure). (The table of this two-dimensional probability distribution is available at *http://www-supernova.lbl.gov/*.) In cosmologies above the near-horizontal line, the universe will expand forever while below this line the expansion of the universe will eventually come to a halt and recollapse. This line is not quite horizontal because at very high mass density there is a region where the mass density can bring the expansion to a halt before the scale of the universe is big enough that the mass density is dilute with respect to the cosmological constant energy density. The upper-left shaded region, labeled "no Big Bang," represents "bouncing universe" cosmologies with no Big Bang in the past. The lower right-shaded region corresponds to a universe that is younger than the oldest heavy elements, for any value of $H_0 \geq 50$ km s^{-1} Mpc^{-1}.

two-filter color measurements to study the possible effect of extinction due to dust that reddens the supernova light, and find that our results are robust with respect to this effect [again, see Perlmutter (Ref. 5) for details].

Our measurements have to be carried out at cosmological distances i.e., large values of z, since for small z values $z < 0.11$, the dependence on Ω is negligible and the luminosity distance becomes $D_L = cz/H_o$.

6. Type Ia Supernovae as Clocks at Cosmological Distances

We will now make use of the "standard" nature of the SNe Ia light curve shapes. This feature allows us to consider the SNe Ia as "clocks" at cosmological distances. As discussed above, SNe Ia are as a class highly homogeneous, since they are thermonuclear explosions that are apparently triggered under very similar physical conditions.

The work of Phillips,[2] Hamuy[14–16] and Riess, Press and Kirshner,[17] have emphasized the *inhomogeneity* of Type Ia light curve shapes, particularly for the "non-normal" redder Type Ia's. Perlmutter[3,5] provided a single-parameter characterization of these light curve differences, which is simply a time-axis stretch factor, s, which stretches (or compresses) the Leibundgut template light curve. From the study based on *nearby* SNe, it was shown that this stretch factor s extends over a range of 0.80 to 1.20 with an occasional outlier outside these values. Light curve shapes have been found to be correlated with peak magnitudes, UV colors, spectral features, etc.[3] We will now show data obtained by treating 36 of these SNe with $0.30 < z < 0.70$ as a group.

Using supernova light curves to test the cosmological expansion was first suggested by Wilson, 1939 (Ref. 18). Over the last decade, it has become clear that SNe Ia are superb and precise clocks, located both nearby and at cosmological distances.

We presented the first clear observation of this time-dilation effect based on our first seven high z type Ia SNe at the 1995 conference at Aigua Blava, Spain, Goldhaber.[19] Later, Leibundgut *et al.*[20] gave confirmatory evidence for time dilation, based on a single, high-z supernova. More recently, Riess *et al.*, 1997 (Ref. 21), showed evidence that the spectral features of SNe Ia can be timed sufficiently well to measure the time interval between two spectra taken ten days apart in the observer system. Applying this method to one SN gave results consistent with the time-dilation factor $1 + z$ at the 96.4% confidence level.

7. Fit to the Light Curve

In our data analysis, we fit each of our observed SNe light curve points to R-band template light curves using the fitting program MINUIT (James and Roos, 1995)[10] . Each R-band template is constructed from the B-band rest system, the Leibundgut template, and the appropriate cross filter K-correction.[11,12]

Each SN is fit for three variables: the day and magnitude of peak light and the width factor $w = s(1+z)$ by which the Leibundgut curve had to be expanded. In the present analysis, we make use of the day at peak to align all the 36 SNe light curves, and we normalize the flux of each SN to unity. As these SNe are measured in the R-band, we now translate the points to the B-band. The individual photometry points are K-corrected[11,12] from the measured R-band photometry points to the B-band, where lower z data is available for comparison.[14–16] Two SNe at $z = 0.18$ and three at $z > 0.7$ have to be K-corrected to the V-band and U-band, respectively, and are thus not included here. One distinct outlier SN97O is also left out here.

8. Analysis of 36 Supernovae Treated as a Group

The stretch factor affects our ability to test time dilation, since the expected dilation factor $1 + z$ is modified by the stretch factor s. The observable effect is then $w = s(1 + z)$. Figure 3(a) shows the distribution of w for SCP data (solid histogram) and Calán/Tololo data (dashed histogram). Figure 3(b) shows the corresponding histograms for s.

If no independent s corrections are made to our width measurements, an additional dispersion of w is observed, assuming a similar population of SNe at high redshift.

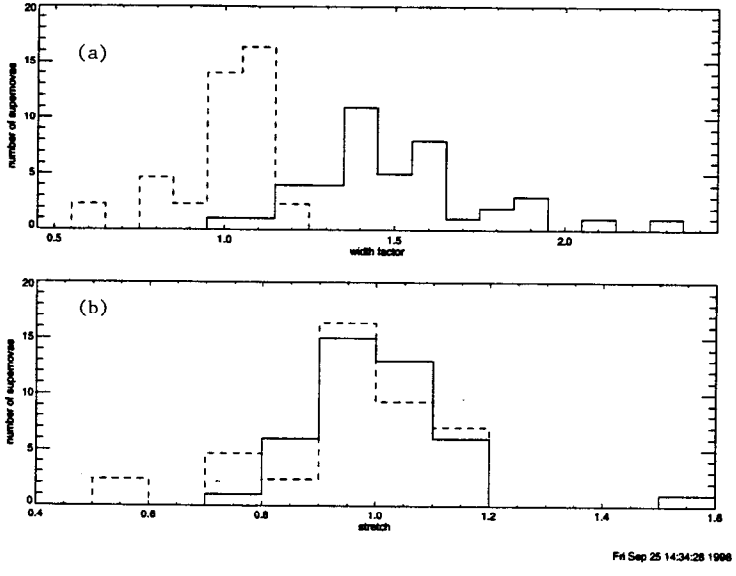

Figure 3: (a) The distribution of the observed light curve width w for the 18 of the Calán/Tololo SNe (broken line histogram) with an area normalized to 42 and the SCP data for 42 fully analyzed SNe (solid line histogram). (b) The corresponding stretch distributions s defined as the observed light curve width divided by $1+z$ for each SN.

Figure 4(a) shows the distribution of w versus $1+z$ for both the Calán/Tololo data and the SCP data. As can be noted, except for two outliers in the SCP data and three in the Calán/Tololo data, $0.8 < s < 1.2$. In Fig. 4(b), we show the stretch distribution s versus $1+z$.

In Fig. 5(a), we show the R-band photometry points, individually K-corrected to the B-band for the SNe with $0.30 < z < 0.70$, aligned at maximum light in the observer system. The measured points for SNe with $0.45 \leq z < 0.70$ are shown in red, the points from SNe with $0.30 < z < 0.45$ are shown in green. Also shown are points (violet) from the 18 SNe from the Calán/Tololo study in the B-band (Hamuy, 1996) with $z < 0.11$, these are also K-corrected. These 18 SNe were chosen out of 29 SNe by having been discovered prior to five days after maximum light. Figure 5(b) shows the same data averaged over all SNe in each z band. Figure 5(b) also shows the same data with the SCP data averaged over the entire $0.30 < z < 0.70$ interval and averaged over two days. Finally, Fig. 5(b) shows the rest system Leibundgut curve extended down to the explosion time (Nugent *et al.*, 1999, Ref. 22, Goldhaber *et al.*, 1999, Ref. 23). These figures illustrate the time dilation effect clearly. The width of the light curves are z dependent in the observer system. The nearby SNe (violet points) approximate the rest system curve, while the high-redshift data (green and red points) give wider distributions. This time dilation is particularly clear in Fig. 5(c). The (violet) low-z points follow the curve while the (green) outer points are clearly much wider, indicating time-dilation.

We now transform the time axis from the observer frame to the rest frame by dividing the appropriate $1+z$ for each data point of each of the SNe, and then divide the time axis by s as well. In Fig. 6(a) and 6(b), we note excellent overlap of all the individual photometry points. Thus with one parameter s and the time dilation $1+z$, all the normalized and aligned SNe fit a single curve. The relations between stretch, color and brightness as noted by Riess *et al.*[19] will be discussed in detail in terms of stretch in an upcoming publication (Kim *et al.*, 1999, Ref. 23).

9. Time Dilation and Doppler Shift–An Example

The time dilation effect can be understood in terms of the Doppler shift. We present a simple example of this.

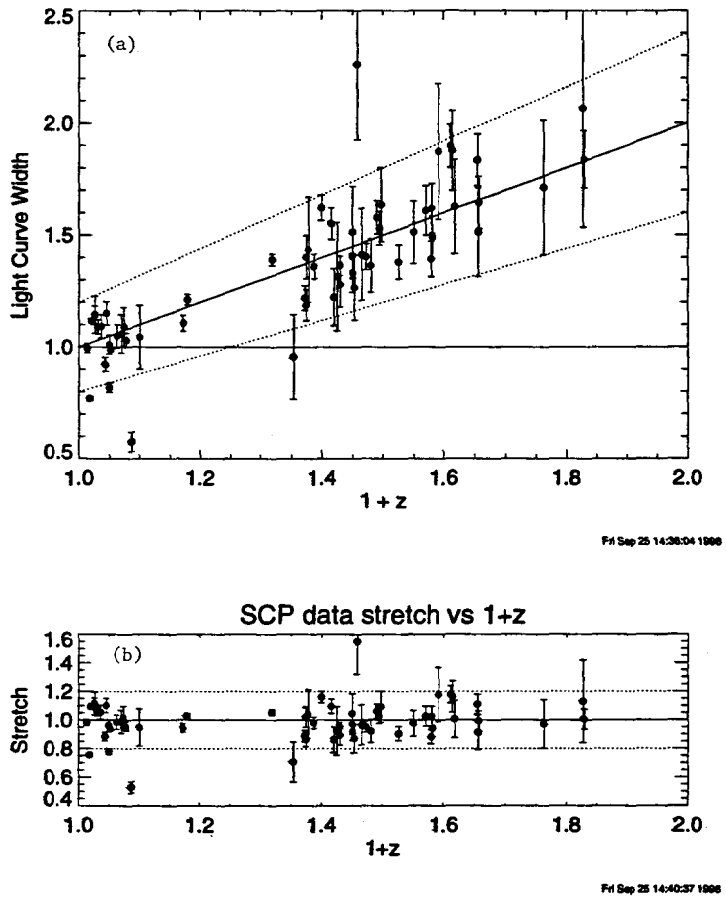

Figure 4: (a) The observed light curve width vs $1+z$. The (violet) points for $z < 0.11$ are the Calán/Tololo SNe, the (red) points for $z > 0.15$ are the SCP data for 42 fully analyzed SNe. The band delineated by the dotted lines corresponds to stretch values 0.8 to 1.2 which encompass the bulk of the data, except for a few outliers. (b) The stretch s vs $1+z$. Stretch is defined as the observed light curve width w divided by $1+z$ for each SN. The points and lines are defined as in (a).

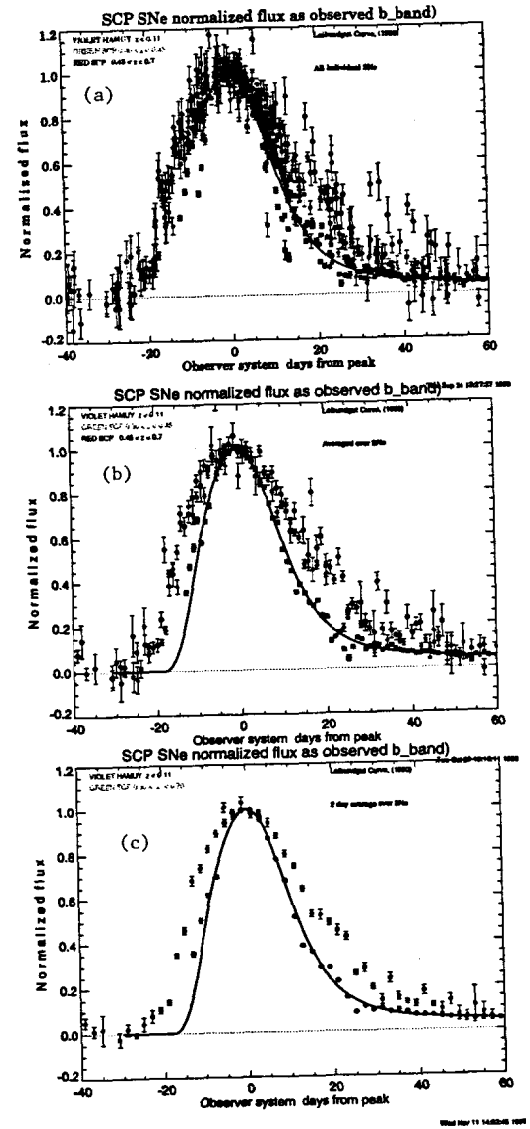

Figure 5: (a) The photometry points for the 34 SCP and 18 Calán/Tololo SNe, flux normalized to unity and aligned at the peak in the observer system. (b) The same data as in (a) averaged over each day. The Leibundgut light curve extended to explosion time[23,24] is also shown, to indicate the rest system. (c) The SCP data for $0.30 < z < 0.70$ and the Calán/Tololo SNe averaged over two days, compared with the extended Leibundgut light curve.

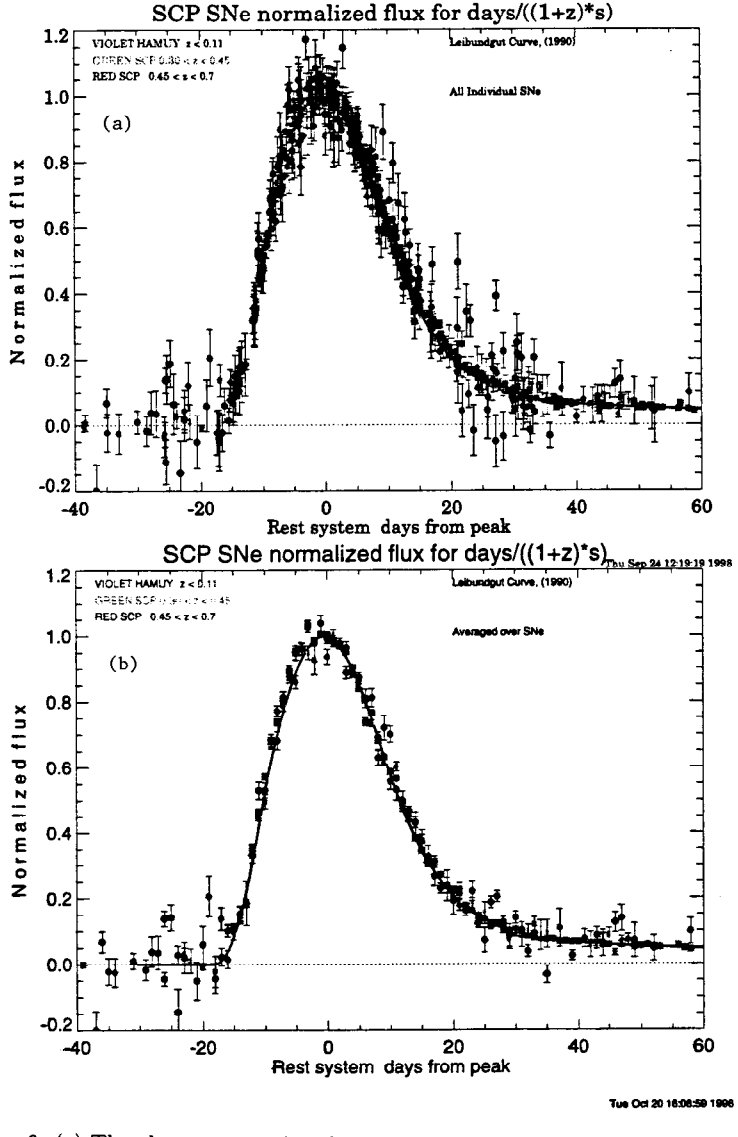

Figure 6: (a) The photometry points for the same three sets of SNe, transformed to the rest system and corrected for the stretch factor s. (b) The same data as in (a) averaged over each day. All the points are consistent with the extended Leibundgut curve[24] indicating that the single parameter s, combined with the expansion factor $1+z$, falls on a unique curve.

We note that the upper limit of the observed redshift $z = 0.7$ corresponds to $\beta = 0.49$ and that $\beta = 0.5$ corresponds to $z = 0.73$. Consider two points in time on the light curve symmetric around the peak and four weeks apart, in the SN rest system for $z = 0.73$. When the light emitted from the first point reaches us, we start our clock in the observer frame. When the light is emitted from the second point the SN will, by the expansion of the universe, be at a greater distance from our telescope. With $\beta = 0.5$, this extra distance will be two light weeks. From this classical effect alone, the two points in the observer system will be six weeks apart, a time dilation of 1.5. Thus, time-dilation measures the expansion of the universe directly. The relativistic version is given by $1 + z = \sqrt{(1+\beta)/(1-\beta)}$ which equals $\gamma(1+\beta)$, where $\gamma = 1/\sqrt{1-\beta^2}$. For the redshift values we are dealing with, the γ factor is only a small correction 1.15 to give 6.93 weeks in the observer frame. The main effect we are observing is thus the direct expansion of the universe. The same argument also holds for the redshift of the light emitted by the SN, where we now think of the two points as two adjacent crests of the light wave.

REFERENCES

1. D. Branch and G.A. Tammann, 1992. Ann. Rev. Astron. Astrophys. **30**, 359–89 (1992).
2. M. M. Phillips, Astrophys. J. **413**, L105 (1993).
3. S. Perlmutter *et al.*, Astrophys. J. **483**, 565 (1997).
4. B. Leibundgut, Supernova, edited by S. E. Woosley (Springer, New York, 1991) 751.
5. S. Perlmutter *et al.*, 1998c. Also available at *www-supernova.LBL.gov* and *astro-ph* (submittted to Astrophys. J.)
6. S. Perlmutter *et al.*, Nature **391**, 51 and erratum (on author list), **392**, 311 (1998a).
7. S. Perlmutter *et al.*, presentation at the *January 1998 Meeting of the American Astronomical Society,* available at *www-supernova.LBL.gov* and *astro-ph*; referenced in Bull. Am. Astron. Soc., vol. 29, p. 1351, 1997, (submittted to Astrophys. J.).
8. A. G. Riess *et al.*, Astrophys. J **116**, 1009 (1998).
9. Norgaard-Nielsen *et al.*, Nature **339**, 523 (1989).
10. F. James and M. Roos, Comput. Phys. Commun. **10**, 343 (1975).
11. A. Kim, A. Goobar, and S. Perlmutter, Publ. Astron. Soc. Pac. **108** 190 (1996).
12. P. Nugent *et al.*, Publ. Astron. Soc. Pac., 1999 (in preparation).
13. A. Goobar, and S. Perlmutter, Astrophys. J. **450**, 14 (1995).

14. M. Hamuy *et al.*, Publ. Astron. Soc. Pac. **105**, 787 (1993).
15. M. Hamuy *et al.*, Astron. J. **106**, 2392 (1993b).
16. M. Hamuy *et al.*, Astrophs. J. **109**, 1 (1995).
17. A. G. Riess, W. H. Press, and R. P. Kirshner, Astrophys. J. **438** L17 (1995). *ibid* **473**, 88 (1996).
18. O. C. Wilson, Astrophys. J. **90**, 634 (1939).
19. Goldhaber, G., *et al.*, in presentations at the *NATO ASI in Aiguablava*, Spain, (1995), LBL-38400, page III.1. Also published in Thermonuclear Supernova, edited by P. Ruiz-Lapuente, R. Canal, and J. Isern; Dordrecht, Kluwer, page 777 (1997).
20. B. Leibundgut *et al.*, Astrophs. J. Lett. **466**, L21 (1996).
21. A. G. Riess *et al.*, Astron. J. **114(2)**, 722 (1997).
22. P. Nugent *et al.*, Astrophys. J., 1999 (in preparation).
23. G. Goldhaber *et al.*, Astrophys. J., 1999 (in preparation).
24. A. Kim, G. Aldering *et al.* Astrophys. J., 1999 (in preparation).